

Convective Initiation

S B Trier, National Center for Atmospheric Research, Boulder, CO, USA

Copyright 2003 Elsevier Science Ltd. All Rights Reserved.

Introduction

Moist convection, which we define as precipitating convection that spans a significant depth of the troposphere, is a phenomenon that can occur almost anywhere on Earth. Moist convection (hereafter referred to simply as convection) is most common over warm, tropical oceanic regions and over continental regions that extend from the Tropics into the mid-latitudes, and assumes a variety of different organizations, ranging from individual ~ 1 – 10 km horizontal scale cumulonimbus clouds to ~ 1000 km horizontal scale mesoscale convective systems (MCSs). Convection affects the atmosphere on a multitude of scales, which range from that of the local surface weather, through heavy rains and occasionally damaging winds, to that of the global circulation, through its aggregate effects on radiation and fluxes of heat, moisture, and momentum.

One of the most difficult aspects of convection to treat theoretically is its initiation. This is due to the many atmospheric processes of varying scales that influence both the vertical thermodynamic structure in which convection occurs and how it is initiated. The background density stratification of the atmosphere tends to resist the vertical displacements that give rise to convection. However, over broad geographical regions the atmosphere is susceptible to convection, given localized upward displacements that are sufficient to allow air to become saturated with respect to water vapor, and ultimately less dense than its surroundings.

In the following, we discuss the thermodynamic vertical structure of the atmosphere and how its ability to support convection may be assessed. We also examine different ways by which the thermodynamic vertical structure can evolve, and thereby allow or prohibit the development of convection. Owing to the vertical stability of the background atmospheric state, the initiation and sustenance of long-lived systems of multiple convective storms typically requires organized vertical motion in the environment. We will review various lifting mechanisms, which vary widely in character from shallow short-lived circulations of limited horizontal scale that are confined within the heated planetary boundary layer (PBL) to the relatively weak, but persistent, larger-scale ascent

that occurs through deep tropospheric layers within mid-latitude cyclones.

Assessment of Vertical Stability

Air Parcels and Conditional Instability

The vertical stability of the atmosphere, and hence its ability to support convection, is often analyzed using the assumptions of the parcel theory. Parcel theory assumes that vertically displaced air does not exchange mass with its surroundings, and instantaneously adjusts to the pressure of the surrounding atmosphere. An air parcel, which may contain water vapor but is initially subsaturated, is also assumed to exchange no heat with its surroundings during its vertical displacement. If displaced upward, the air parcel will cool at the dry adiabatic lapse rate $\Gamma_d \equiv -dT_p/dz = g/c_p \sim 10 \text{ K km}^{-1}$, where T_p is the air parcel's temperature, $-g$ is the acceleration due to gravity, and c_p is the specific heat at constant pressure.

When an air parcel is given a vertical displacement, its direction of subsequent vertical acceleration depends upon its buoyancy, given by eqn [1].

$$B = g \frac{[\theta_{vp}(z) - \theta_v(z)]}{\theta_v(z)} \quad [1]$$

In eqn [1], $\theta_{vp}(z)$ is the virtual potential temperature of the air parcel (*see Thermodynamics: Moist (Unsaturated) Air*) and $\theta_v(z)$ is the virtual potential temperature of the environment. In the statically stable atmosphere ($\Gamma \equiv -\partial T/\partial z < \Gamma_d$), an air parcel that remains subsaturated during its vertical displacement will become negatively (positively) buoyant if displaced upward (downward) from its original position and will thus tend to return to its original position.

Since the air parcel conserves its mixing ratio q , if it is given a sufficient upward displacement it will eventually become saturated as a result of its adiabatic cooling. The level at which this occurs is referred to as either the lifting condensation level (LCL) or the convective condensation level (CCL), depending on whether the parcel displacement results from mechanical lifting or turbulent circulations forced by surface heating, respectively. Once saturated, the ascending air parcel cools less rapidly, owing to latent heat release from condensation. Parcel theory predicts that the saturated air parcel cools at the moist adiabatic lapse rate, Γ_s (*see Thermodynamics: Saturated*

Adiabatic Processes), which ranges from $\sim 4 \text{ K km}^{-1}$ for warm conditions in the lower troposphere to close to $\Gamma_d \sim 10 \text{ K km}^{-1}$ near the tropopause.

When the lapse rate of an atmospheric layer falls between that of Γ_d and Γ_s , the layer is conditionally unstable. The instability is conditional in the sense that upward vertical displacement must be sufficient to saturate the air parcel, whereby its reduced rate of cooling upon subsequent ascent would allow it eventually to become positively buoyant.

Figure 1 presents examples of conditionally unstable atmospheric soundings that are representative of conditions that can occur over the central United States during the warm season (Figure 1A) and over a tropical oceanic region (Figure 1B), where the seasonal variations in temperature are less. In these diagrams, ascent curves, based on the assumptions of parcel theory, are plotted for the most conditionally unstable air, which is situated within the PBL for each case. Because of the lower relative humidity in the mid-latitude PBL, air from within its lowest 50 hPa must rise a significantly greater distance to reach the LCL than in the tropical case. Moreover, a 75 hPa deep stable layer surmounts the PBL in the mid-latitude case (Figure 1A). These two conditions necessitate much deeper lifting for this air (Figure 1A) to reach its level of free convection (LFC), where the air parcel becomes warmer than the environment (and hence positively buoyant) than in the tropical case (Figure 1B). However, the environmental lapse rate, Γ , within the mid-troposphere is considerably larger in the mid-latitude case (Figure 1A) than in the tropical case (Figure 1B), where it is close to Γ_s (moist adiabatic). This results in significantly greater maximum parcel buoyancy [1] in the mid-latitude case, where the bold gray curves in Figure 1 indicate a greater maximum parcel temperature excess over its environment, which also implies a greater virtual potential temperature excess, since $\theta_v = \theta(1 + 0.61q)$.

Convective Available Potential Energy

A useful measure of the maximum possible intensity of convection is the convective available potential energy, CAPE, given by eqn [2].

$$\text{CAPE} = \int_{\text{LFC}}^{\text{LNB}} B \, dz \quad [2]$$

CAPE is the parcel buoyancy, B , vertically integrated between the LFC (Figure 1) and the level of neutral buoyancy (LNB), at which the parcel ceases to have a virtual potential temperature excess over that of the environment (Figure 1), and thus decelerates vertically. The maximum vertical velocity an air parcel may

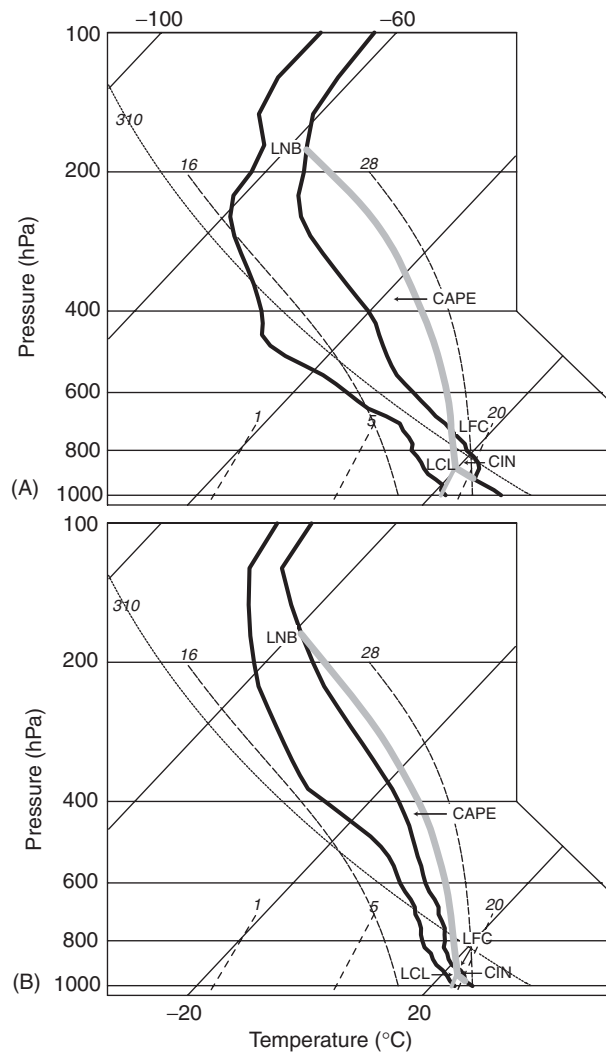


Figure 1 Skew T - $\log P$ diagrams for conditionally unstable (A) warm-season continental midlatitude and (B) oceanic tropical environments. The solid black curves indicate environmental temperature (right) and dewpoint (left), whereas the heavy gray curve represents the hypothetical temperature of an ascending air parcel whose initial mixing ratio and potential temperature are averages of these environmental quantities in the lowest 50 hPa. Note that the parcel ascends along a dry adiabat (constant θ) below its LCL (see text for explanation), and along a moist adiabat (constant θ_w) above its LCL (see text for explanation). Locations of positive CAPE, where parcel temperature excess occurs between the LFC and LNB (see text for explanation), and CIN, where parcel temperature deficit occurs beneath the LFC (see text for explanation) are indicated by arrows. The plot background consists of the $p = 1000, 800, 600, 400, 200,$ and 100 hPa isobars (thin horizontal lines), $T = -100, -60, -20,$ and 20°C isotherms (45° skewed thin solid lines), $q = 1, 5,$ and 20 g kg^{-1} isohumes (long-dashed thin solid lines), $\theta_w = 16^\circ\text{C}$ and 28°C moist adiabats (medium-dashed lines), and the $\theta = 310 \text{ K}$ dry adiabat or isentrope (dotted pattern).

achieve, w_{\max} , may be estimated by substituting the form of the vertical momentum equation derived from parcel theory, $dw_p/dt = w_p(dw_p/dz) = B$, into eqn [2] and taking the square root, which yields

$w_{\max} \equiv w_p(z = \text{LNB}) = (2\text{CAPE})^{0.5}$. For the CAPE of $2750 \text{ m}^2 \text{ s}^2$ in the example mid-latitude sounding (Figure 1A), $w_{\max} \sim 74 \text{ m s}^{-1}$, whereas, for the CAPE of $1000 \text{ m}^2 \text{ s}^2$ in the tropical sounding (Figure 1B), $w_{\max} \sim 45 \text{ m s}^{-1}$. Note however, that w_{\max} represents only an approximate upper bound on the actual maximum vertical velocities. Typically, downward-directed pressure gradient forces, and negative contributions to the buoyancy that result from condensate in updrafts and entrainment of environmental air (each of which are neglected by parcel theory), significantly reduce the vertical velocities. Parcel theory will most significantly overestimate w_{\max} for soundings resembling the tropical case (Figure 1B), since entrainment and condensate loading generally have a greater percentage effect on smaller parcel buoyancies.

On the skew-T diagram of Figure 1, the CAPE is proportional to the area between the parcel ascent curve and environmental temperature curve between the LFC and LNB. Thus, for a given environmental vertical profile of temperature or potential temperature, the CAPE has a unique dependence on the moist adiabat along which the positively buoyant air parcel ascends. The moist static energy, $h = gz + c_p T + Lq$, is conserved along a moist adiabat. Thus, since c_p is a constant and L has only a weak dependence on T , equivalence of the thermal and moisture contributions to CAPE may easily be established. For example, a moisture increment of $\Delta q = 1 \text{ g kg}^{-1}$ has the same approximate effect on CAPE as a temperature increment of $\Delta T = 2.5 \text{ K}$.

Convective Inhibition

Although the CAPE provides a measure of how strong convection can become, it provides no guidance on whether it will actually occur. Indeed, expansive regions may have positive CAPE, but the areas experiencing convection at any given time are considerably smaller. This is because there is usually an energy barrier that has to be overcome before convection can occur. This energy barrier, referred to as the convective inhibition (CIN), corresponds to the negative area on the skew-T diagram beneath the LFC (Figure 1), and represents the work needed to be done on the conditionally unstable air parcel for it to reach its LFC. Thus, provided CAPE exists, CIN is the quantity most critical to convective initiation.

The analysis of how CIN is influenced by the thermal and moisture characteristics of an air parcel is more complicated than for CAPE, since CIN does not depend uniquely on the moist static energy of the air parcel. The sensitivity of CIN to changes in temperature and moisture depends on the details of the sounding. For the simple (but frequently observed)

case of a well-mixed PBL within which θ and q are approximately constant, a temperature change of ΔT will have a greater effect on the CIN than a mixing ratio change of Δq that corresponds to the same increment of moist static energy Δh . This dependence of CIN on temperature and moisture is illustrated schematically in Figure 2. Since the moist adiabat along which the air parcel (once saturated) will ascend is the same for equivalent changes in temperature or moisture, the greater sensitivity of CIN to changes in temperature results from the additional changes in CIN for the unsaturated portion of the lifting (compare Figures 2B and 2C).

Returning to the example soundings from different geographical regions, we find that, despite having a greater CAPE than the tropical sounding, and thus a greater potential for intense convection, the mid-latitude sounding has a significantly larger CIN of $110 \text{ m}^2 \text{ s}^2$ (Figure 1A) versus $10 \text{ m}^2 \text{ s}^2$ for the tropical sounding (Figure 1B). It is not unusual for the most conditionally unstable soundings to have substantial amounts of CIN, for it is the energy barrier to convection that is often largely responsible in allowing large values of CAPE to develop and persist.

In the absence of persistent forcing, an initial vertical velocity of $w = (2\text{CIN})^{0.5}$ is required to displace an unsaturated air parcel to its LFC. For the CIN of $110 \text{ m}^2 \text{ s}^2$ in the example mid-latitude sounding (Figure 1A), this vertically velocity is $w \sim 15 \text{ m s}^{-1}$. Vertical velocities of this magnitude are rarely observed outside of convection, which underscores the necessity of mechanism(s) that reduce the CIN prior to the development of convection. These factors are explored in some detail in subsequent sections.

Potential Instability and Equivalent Potential Temperature

So far, we have considered the susceptibility to convection when idealized parcels of air undergo vertical displacements in a subsaturated environment. The theory of conditional instability of air parcels makes no assumptions on the evolution of the vertical structure of the atmosphere and, by itself, may be most germane to the development of convection over localized regions, where either the CIN has been diminished and/or there exists strong forcing that is capable of displacing initially subsaturated air to its LFC. However, there are situations in which convection can develop simultaneously over broad (e.g., $\sim 100\text{--}500 \text{ km}$) regions as a result of the widespread lifting of deep atmospheric layers. The development of convection under these circumstances may be best described using the concept of potential instability. In an environment that is potentially unstable, it may be

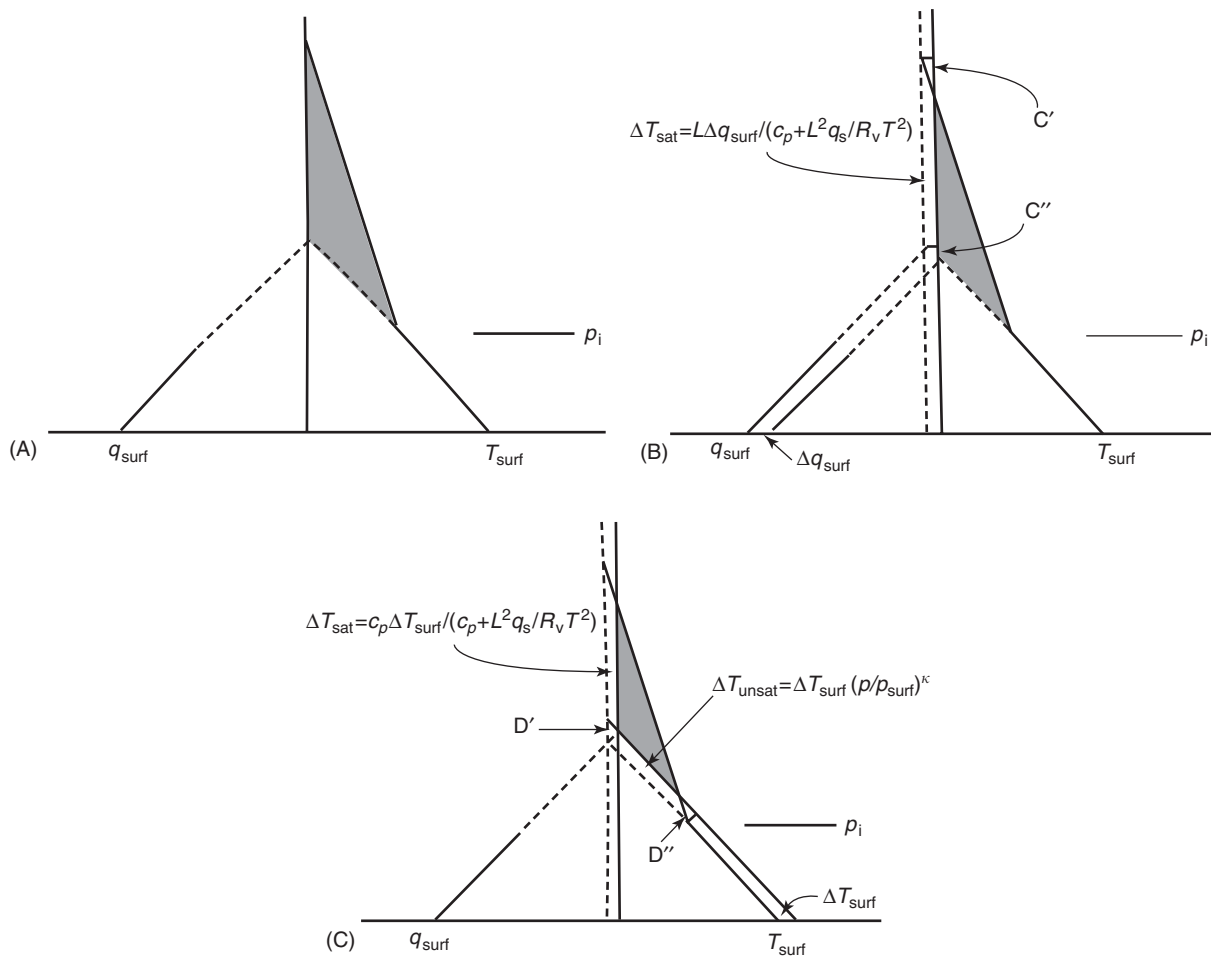


Figure 2 Schematic diagram illustrating the influence of PBL (B) mixing ratio increases Δq_{surf} , and (C) temperature increases, ΔT_{surf} , on the CIN of panel (A). In each panel, CIN is indicated by the area of the shaded region and the top of the unmodified PBL is indicated by the pressure p_i . In both panels (B) and (C), the moist adiabat of the unmodified PBL is indicated by the vertical dashed line, whereas the moist adiabat of the modified PBL is indicated by the vertical solid line. In panels (B) and (C), the respective differences between the areas C' and C'' , and areas D' and D'' are small compared to the changes in CIN from panel (A) to each of these other panels. Note that in panel (B) the decrease in CIN from that of panel (A) is due solely to the increase in PBL moisture in the saturated portion of lifting, whereas in panel (C) the decrease in CIN from that of panel (A) also depends on the temperature increase in the unsaturated region, ΔT_{unsat} . (Adapted from Crook (1996).)

possible, through lifting, to create layers that are saturated and also have lapse rates greater than Γ_s , regardless of the initial thermal stratification of the layer. When this occurs, convection may erupt from within the saturated layer, which has zero CIN and is absolutely unstable.

Potential instability is defined using the thermodynamic field variable of equivalent potential temperature θ_e , which is the potential temperature an air parcel would have if all its water vapor were condensed and the resulting latent heat were used to warm the parcel. Large values of both θ and q contribute to large values of θ_e . The criterion for potential instability is the decrease of equivalent potential temperature with height, $\partial\theta_e/\partial z < 0$. Typically, the largest θ_e

occurs in the PBL, with a broad minimum in the middle troposphere. This stratification of θ_e supports potential instability through much of the lower troposphere.

Thermodynamic Destabilization Processes

Accurate forecasting of convective initiation is confounded by the availability of vertical profiles of temperature and moisture variables at only limited frequency and horizontal resolution. In practice, knowledge of physical processes must be used to anticipate the local evolution of thermodynamic stability.

Both the CAPE and CIN are sensitive to the lower-tropospheric moisture, which, excluding phase changes within a lower-tropospheric volume, evolves according to the relation

$$\frac{\partial q}{\partial t} = (-\mathbf{v} \cdot \nabla_{\mathbf{h}} q) - w \frac{\partial q}{\partial z} - \nabla_{\mathbf{h}} \cdot (\mathbf{v}'q') - \frac{\partial}{\partial z} (w'q') \quad [3]$$

In eqn [3], the local change of mean mixing ratio q depends on horizontal and vertical advectations of its mean component, and on the horizontal and vertical flux convergences of its eddy component q' .

Given sufficient lower-tropospheric moisture for CAPE to exist, both CIN and CAPE are sensitive to the lapse rate of temperature. The local change of lapse rate, given by eqn [4], is influenced by the differential diabatic heating rate, differential temperature advection, and the adiabatic temperature changes due to vertical motion, which respectively comprise the three terms on the right side of eqn [4].

$$\begin{aligned} \frac{\partial \Gamma}{\partial t} &\equiv \frac{\partial}{\partial t} \left(-\frac{\partial T}{\partial z} \right) \\ &= -\frac{1}{c_p} \frac{\partial Q}{\partial z} - \frac{\partial}{\partial z} (-\mathbf{v} \cdot \nabla_{\mathbf{h}} T) + \frac{\partial}{\partial z} [w(\Gamma_d - \Gamma)] \quad [4] \end{aligned}$$

Forecasting the evolution of thermodynamic stability is challenging, since two or more simultaneous processes that influence the vertical temperature and moisture structures may have significant, but sometimes canceling, effects. In the following, we describe processes that can lead to thermodynamic destabilization (i.e., increases in CAPE and/or decreases in CIN).

Turbulent Heat and Moisture Fluxes

The lower troposphere is strongly influenced by the diurnal cycle of surface heating. During the day, the air in contact with the heated ground warms by conduction. This results in a decrease in stability of the lowest layers through the differential diabatic heating term (first term on the right-hand side of eqn [4]). However, the evolution of the PBL temperature structure, initiated by the surface heating, is a complex process influenced by turbulent eddies (thermals) that mix with air of higher potential temperature at successively higher altitudes. This extends the depth of the neutral (dry adiabatic) layer during the day (Figure 3). The rate of destabilization of the lapse rate ($\partial \Gamma / \partial t > 0$) and growth of the PBL depends on several factors, including the vigor of the vertical motions within the turbulent eddies and the stability of the air above the PBL. At night, the surface heat loss due to infrared radiation increases the stability of the PBL.

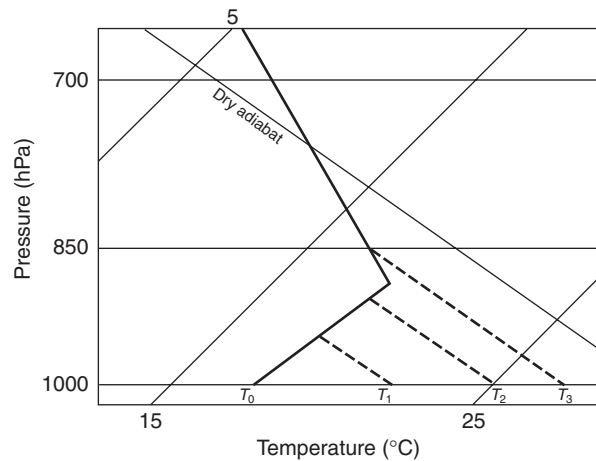


Figure 3 Idealization of how surface heating alters the lapse rate (dashed curves) of the lower troposphere from early morning conditions (solid curve).

Unlike potential temperature, θ , mixing ratio usually decreases with height. In a well-mixed daytime PBL, water vapor is transported upward and drier air is transported downward within turbulent eddies such that $\overline{(w'q')} > 0$. When drier air is entrained into the PBL faster than it can be replaced by evaporation at the surface, the eddy vertical moisture flux divergence (fourth term on the right-hand side of eqn [3]) forces a decrease of q within the PBL. This is often the case over land when there is both a decrease in q and a lack of a strong stable layer above the PBL. Within the warming and drying PBL that can occur in this situation, CIN typically decreases and, in some cases, may be eliminated entirely. However, the CAPE may also decrease when there are sharp decreases in q above the PBL, such that the resulting PBL decreases in q from $-\partial(w'q')/\partial z < 0$ overwhelm the PBL increases in θ that arise from eddy vertical heat flux convergence, $-\partial(w'\theta')/\partial z > 0$. In other situations, such as cases of either strong stability above the PBL or enhanced evaporation at the surface, the latter of which can occur over warm tropical oceanic regions, and when cold air masses encounter warm ocean currents or pass over unfrozen lakes, the sensible heat and moisture fluxes typically act together to increase the PBL CAPE.

Horizontal Advectations

Differential temperature advection, in which more rapid cooling (warming) occurs at upper (lower) levels, will contribute to the destabilization of lapse rates through the second term on the right-hand side of eqn [4]. In the middle latitudes, this often occurs within the warm sector of baroclinic waves, both ahead of surface cold fronts and upper-level

shortwaves and within lower-tropospheric warm frontal zones. In these environments, where a significant component of the lower-tropospheric temperature advection is geostrophic, the regions of maximum lower-tropospheric warm advection often experience large-scale (e.g., quasi-geostrophic) ascent, which may also contribute the destabilization of the lapse rate through the third term on the right-hand side of eqn [4].

In some cases, lower-tropospheric warm advection may be accompanied by positive horizontal moisture advection (First term on the right-hand side of eqn [3]). The simultaneous local lower-tropospheric temperature and mixing ratio increases can result in dramatic increases in CAPE, with decreases in CIN.

Vertical Motions

Vertical motions can contribute to thermodynamic destabilization in several ways. In a statically stable environment ($\Gamma < \Gamma_d$), upward motion results in adiabatic cooling. Thus, when vertical motion occurs above a conditionally unstable layer, such as the daytime PBL, it increases the CAPE and reduces the CIN of this layer through adiabatic temperature changes aloft. Since large-scale ascent generally increases with height in the lower troposphere, in addition to cooling deep layers above the PBL, such lifting has a tendency to both raise and weaken preexisting stable layers through the third term on the right-hand side of eqn [4]. Persistent large-scale lifting is particularly effective in reducing CIN, when combined with the more intense turbulent vertical motions generated by surface heating, which increase the potential temperature of the PBL. In contrast to large-scale ascent, large-scale subsidence tends to both intensify stable layers and lower their height, which is deleterious to convective initiation. In tropical regions, vertical motions are crucial in influencing adiabatic temperature changes, since horizontal temperature advectations are considerably weaker than those found in mid-latitudes.

Adiabatic cooling from upward motion is often accompanied by moistening from vertical advectations (Second term on the right-hand side of eqn [3]). Given sufficiently moist initial conditions, persistent large-scale ascent can saturate lower-tropospheric layers. This represents a second way in which vertical motions can contribute to thermodynamic destabilization. Since the strongest mesoscale or synoptic-scale ascent most often occurs above the maximum lower-tropospheric θ_e , which is typically located within the PBL, CAPE within these saturated layers is often less than for the unsaturated air of the PBL. However, in contrast to the conditionally unstable PBL, the layer

saturation may result in absolute instability, which obviates the need for additional forcing to displace air to its LFC. An example of an elevated, approximately saturated layer that resulted from persistent lower-tropospheric ascent of potentially unstable air is shown in **Figure 4**. Here, air originating at 870 hPa that undergoes an average ascent of $\sim 2 \text{ cm s}^{-1}$ explains the approximately saturated condition at 800 hPa 12 h later. Following the lifting, modest (but not insignificant) CAPE of $200\text{--}1200 \text{ m}^2 \text{ s}^{-2}$, with negligible CIN, exists within the 870–770 hPa moist layer.

Convective Initiation Mechanisms

Although the decrease of CIN can be accomplished by processes that do not directly involve vertical motions, environmental lower-tropospheric ascent (at some horizontal scale) is generally required both to initiate convection and to allow it to persist significantly

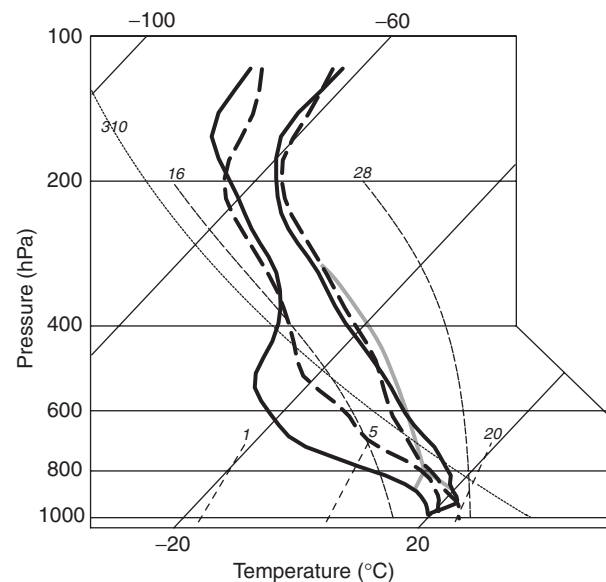


Figure 4 Skew T -log p diagram illustrating the effect of persistent, weak mesoscale ascent on the evolution of temperature and moisture within the approximate 900–700 hPa layer. Solid (dashed) black lines represent the temperature and dewpoint soundings at the beginning (end) of a 12 h trajectory of an air parcel that begins at 870 hPa and ends at 800 hPa. Since potential temperature and mixing ratio are approximately conserved along this trajectory (as indicated by the gray parcel ascent curves), temperature and relative humidity changes along the trajectory between 870 hPa (solid) and 800 hPa (dashed) are due almost entirely to vertical displacement along the trajectory. The moist adiabat along which the approximately saturated 800 hPa air parcel would further ascend is also plotted in gray. The plot background is as in **Figure 1**. (From Trier SB and Davis CA (2002) Influence of balanced motions on heavy precipitation within a long-lived convectively generated vortex. *Monthly Weather Review* 130.)

beyond the lifetime ($\tau \sim 1$ h) of a single cumulonimbus cloud. Possible exceptions may be forms of propagating convection (e.g., supercells and squall lines) that develop in strong vertical shear. Here, convection may persist through the interactions of its own internal circulations with the environmental vertical shear (*see Convective Storms: Overview*). However, even in these cases, convective initiation probably results directly from lower-tropospheric ascent. A comprehensive description of the full range of lifting mechanisms and their detailed dynamics is beyond the scope of the current discussion. What follows is a qualitative overview of several broadly defined classes of lifting mechanisms commonly associated with convective initiation.

Forced Mesoscale Ascent

Isentropic mesoscale ascent, which occurs under conditions of warm horizontal temperature advection, can play an important role in convective initiation in two different ways. It may directly initiate convection by saturating conditionally or potentially unstable lower-tropospheric layers, or it may simply contribute to the reduction of CIN, which determines where more intense and fine-scale PBL-based lifting mechanisms initiate the convection. Isentropic mesoscale ascent may be orographically forced or associated with the overrunning of statically stable air masses.

One example of isentropic mesoscale ascent is that which arises from the interaction of a vortex with the ambient vertical shear. The idealized lifting pattern associated with a convectively generated mesoscale vortex (MCV) is shown in Figure 5. Here, lower-tropospheric air flows up (down) the isentropes downshear (upshear) of the vortex (Figure 5A). There is also an additional component of isentropic vertical motion associated with tangential component of the vortex flow if the ambient vertical shear is thermally balanced (Figure 5B).

Isentropic mesoscale ascent is often manifested as relative flow up frontal surfaces. Low-level jets (LLJs) of high- θ_e air that encounter quasi-stationary surface fronts constitute an example in which the frontal lifting may help initiate convection. These LLJs, which have a significant poleward component, are common leeward of major north-south oriented mountain chains (e.g., the Rockies and Andes mountains), and are enhanced at night for a variety of reasons, including the cessation of surface drag during the evening and the development of thermally driven circulations associated with sloping terrain. The interaction of nocturnal LLJs with quasi-stationary fronts may account for the development or persistence

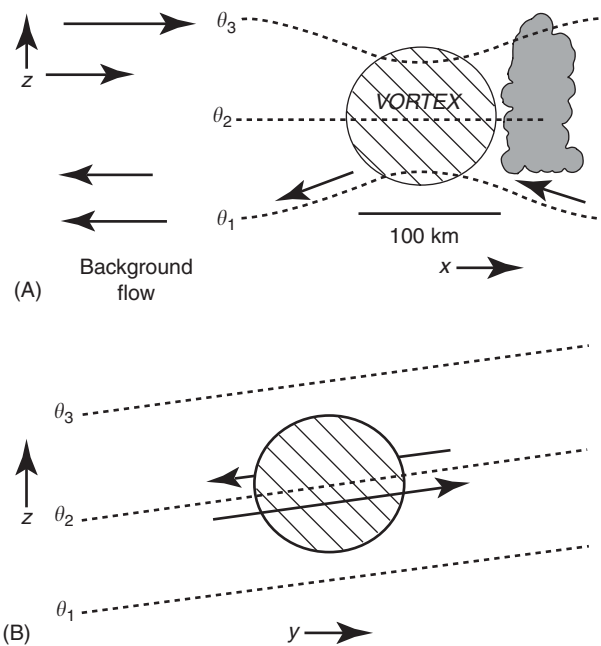


Figure 5 Schematic diagram illustrating isentropic (i.e., dry adiabatic) lifting in the vicinity of an MCV, idealized as a steady, balanced positive potential vorticity anomaly (hatched region) in ambient vertical shear. (A) Upglide associated with the background vertical shear along isentropic surfaces (surfaces of constant potential temperature) deformed by the vortex, and (B) vortex-induced motion along the isentropic surfaces of the background baroclinic zone (From Trier SB, *et al.* (2000) Long-lived mesoconvective vortices and their environment. Part I: Observations from the central United States during the 1998 warm season. *Monthly Weather Review* 128: 3376–3395, which was based on Raymond DJ and Jiang H (1990) A theory for long-lived mesoscale convective systems. *Journal of the Atmospheric Sciences* 47: 3067–3077.)

of a substantial fraction of the large nocturnal MCSs observed during the warm season over the central United States.

Solenoidal Circulations

Solenoidal circulations comprise a broad class of thermally direct atmospheric flows (in which warm air rises and cold air sinks) forced by baroclinity, $(R/p)\nabla p \times \nabla T \neq 0$. They may range in horizontal scale from that of the atmosphere's general circulation to highly localized ($L \sim 1$ – 10 km) circulations confined to the PBL. Lower-tropospheric solenoidal circulations often result from differential surface heating. Under hydrostatic conditions, their strength is proportional to the magnitude of the temperature gradient on a horizontal surface and the depth through which the temperature gradient extends. Differential surface heating has a variety of causes including sloped or irregular terrain, land-water contrasts, land

surface contrasts (e.g., vegetative differences), horizontal gradients in soil moisture, and spatial variations in cloudiness. The two most widely documented thermally induced solenoidal circulations are land/sea breezes and mountain/valley circulations.

Sea breezes are common during the warm season when large temperature differences occur between sea and land surfaces during the late morning and afternoon. In the absence of strong synoptic offshore flow, the cooler and denser air that originates over the sea surface flows inland along the surface temperature gradient (Figure 6) (If the sea breeze persists for a significant portion of the inertial period, $1/f$ seconds, it may develop a substantial alongshore component due to the Coriolis force.) Ascent of the warmer and more buoyant air that originates over land occurs at the sea breeze boundary and may initiate convection. Over warm seas, convection may initiate offshore at night owing to the diurnally reversing surface temperature gradient.

In the mountain/valley circulation, during the day elevated terrain is heated more rapidly than the surrounding atmosphere at the same elevation. This induces an upslope flow, with ascent occurring over the higher terrain. Combined ascent and upslope transport of water vapor is one of the reasons why the first convective initiation tends to occur earlier in the day in mountainous terrain than over adjacent flatlands. In addition to the thermally induced convergence zones that occur in the vicinity of elevated

terrain, mechanically induced convergence zones that result from blocking of the ambient flow by the terrain may also serve as sites for convective initiation.

Solenoidal circulations may also be associated with temperature (density) contrasts arising from antecedent convection. In particular, deep convection is often initiated along the leading edge of evaporatively chilled thunderstorm outflows, which are sometimes referred to as ‘gust fronts’. Gust fronts are often evident as fine lines of weak radar reflectivity on Doppler radar displays or as a narrow band of cumulus clouds in visible satellite imagery, and have depths ranging from a few hundred meters to a few kilometers above the surface. Strong nonhydrostatic vertical pressure forces may lead to intense vertical accelerations within a narrow horizontal band (~ 1 km) along the leading edge of the stronger and deeper gust fronts, which can result in conditionally unstable air being lifted to its LFC (Figure 7).

Generally speaking, fine-scale PBL-based circulations are particularly effective in initiating convection not only because of the intensity of their vertical motions ($w \sim 1\text{--}10 \text{ m s}^{-1}$) but also because of their location in the lowest few kilometers, where the most conditionally unstable air typically exists. In the case of gust fronts, convective initiation is most favored when either two or more of them collide or when one of them collides with or intersects a thermal or kinematic boundary of some other origin. The leading edges of synoptic cold fronts or sea breeze fronts that have undergone frontogenesis (see **Frontogenesis**) and possess concentrated surface temperature gradients and windshifts may behave similarly to gust fronts.

Drylines

Drylines are a phenomenon whose formation arises not only from PBL processes but also from synoptic-scale advective processes. Unlike the aforementioned sources of solenoidal circulation associated with convective initiation, drylines are not typically characterized by large surface density or temperature gradients but, rather, by large surface moisture gradients. Drylines are most common during spring and early summer, and occur over regions where sources of plentiful water vapor (e.g., air originating over a large, warm water body) and dry air (e.g., air originating over a large elevated plateau) are juxtaposed. The dryline that is intermittently present over the southern plains of the United States is a well-known initiation site for severe convective storms. At present, the mechanism(s) for convective initiation along drylines

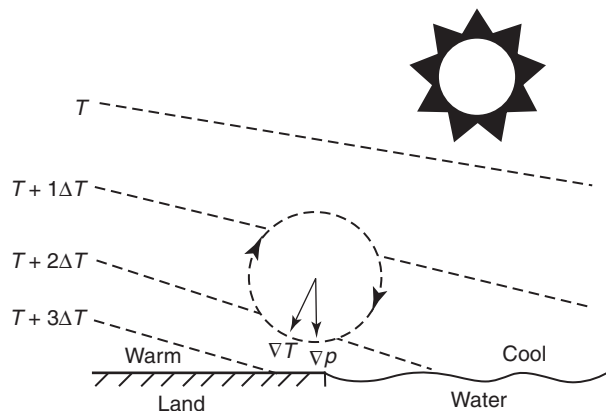


Figure 6 Schematic diagram indicating the solenoidal circulation forced by shallow baroclinity at a coastline where land–sea temperature contrasts occur during the day. The thin dashed lines are isotherms, and the dashed loop with large heads indicates the sense of the circulation. Here, the horizontal component of flow is directed onshore at lowest levels, with ascent over the warmer land surface. The directions of the temperature and pressure gradient vectors, whose displacement from each other accounts for the circulation, are indicated by the arrows with small heads.

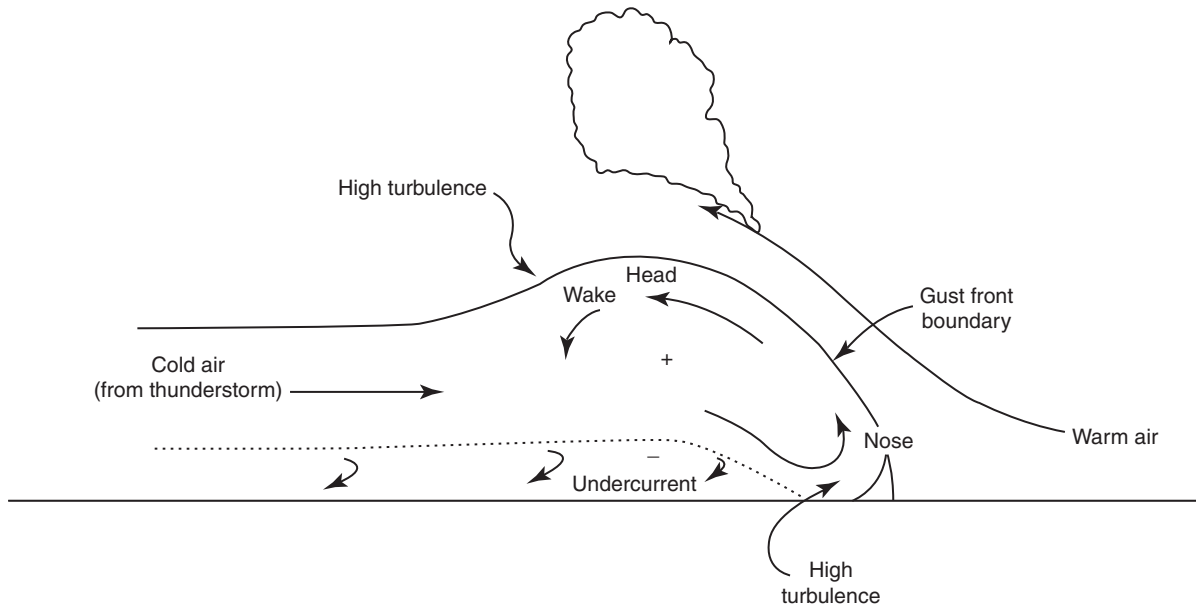


Figure 7 Schematic diagram of thunderstorm outflow derived using measurements from an instrumented tower. Strong forced ascent of warm air at the leading edge of the outflow results in the development of a cumulus cloud, which, depending on the stratification above, could become a new thunderstorm. (Modified with permission from Goff, RC (1976) Vertical structure of thunderstorm outflows. *Monthly Weather Review* 104: 1429–1440.)

are not completely understood and may vary from case to case. In some cases convection initiates during the daytime along drylines that exhibit strong horizontal convergence across the surface moisture gradient, owing to enhanced downward transports of momentum within the drier air where the PBL depth is greater.

Gravity Waves and Related Phenomena

Disturbances to a stably stratified fluid result in oscillations, known as gravity (buoyancy) waves, in which buoyancy is the restoring force (*see Dynamic Meteorology: Waves*). The vertical displacements associated with mesoscale gravity waves have been hypothesized to influence the initiation of convec-

tion. Disturbances that initiate gravity waves in the atmosphere are varied and include the diabatic heating that occurs in MCSs. This heating creates an imbalance between the mass and wind fields, which the atmosphere adjusts to by simultaneous emission of transient gravity waves and the development of longer-lived rotational (balanced) flows such as MCVs. A vertical profile of diabatic heating similar to that of an MCS dominated by a large region of stratiform precipitation produces gravity waves that cause upward displacements in the lower troposphere of the nearby atmosphere. These upward displacements may be sufficient to destabilize oceanic tropical environments that possess relatively small CIN, and have been hypothesized to explain the observation of the frequent development of new

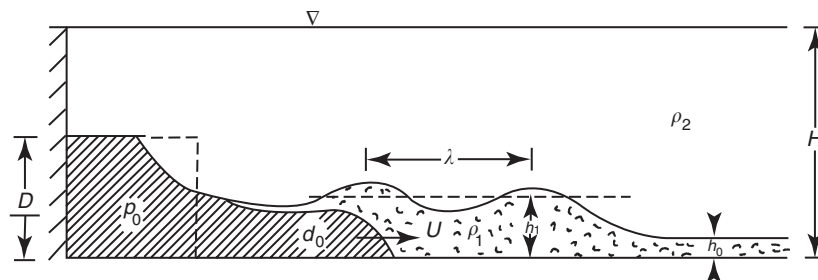


Figure 8 Schematic illustration of an internal bore of wavelength λ and depth h_1 generated by the advance of a density current of depth d_0 into the denser fluid (ρ_1) of undisturbed depth h_0 within the two-fluid system ρ_1, ρ_2 . (Modified with permission from Simpson (1997).)

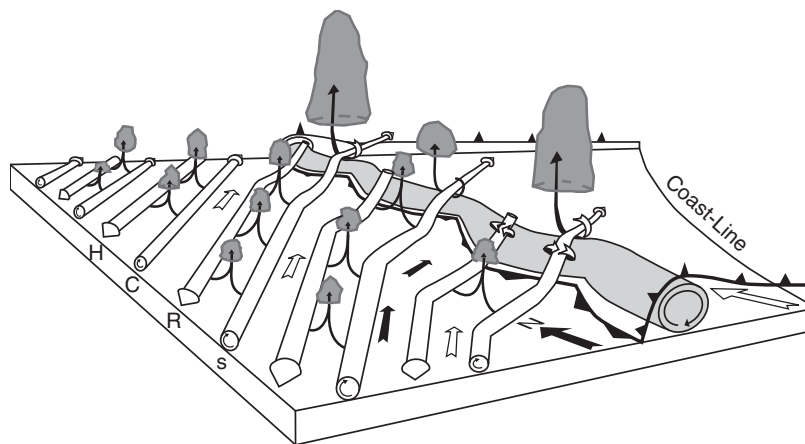


Figure 9 Schematic diagram showing interaction between the sea-breeze front and HCRs and how it relates to cloud development. The sea-breeze front is delineated by the heavy, barbed line. The circulation at its leading edge is lightly shaded. The horizontal vorticity vectors associated with counterrotating roll circulations are shown. Clouds along the HCRs and at the intersection points along the front are shaded in gray. The shear vector (solid, 2D arrow) and the low-level winds (white, 2D arrow) are also shown. (From Atkins NT *et al.* (1995) *Monthly Weather Review* 123: 944–969.)

cloud clusters in close proximity to preexisting cloud clusters within parts of the intertropical convergence zone.

In addition to the example of a deep gravity mode discussed above, gravity waves and related phenomena may be excited when an outflow from antecedent convection encounters a layer of strong stability (Figure 8). The stably stratified nocturnal PBL provides an example of a medium in which these shallow disturbances may maintain coherence as they propagate. In some instances the vertical displacements associated with these and similar ‘trapped’ disturbances may initiate new convection, provided that sufficiently moist and unstable air is situated above the stable layer.

Turbulent PBL-based Circulations

When there is little or no CIN for air within the PBL, thermally driven PBL turbulence may determine where convection first initiates. This is due not only to the inhomogeneities in vertical motions within the turbulence but also to differences in vertical stability. For example, observational studies of horizontal convective roll (HCR) circulations, which are generally aligned along the PBL vertical shear vector and have horizontal wavelengths of 5 km or less, indicate significant differences in PBL temperature and moisture content depending on whether measurements were taken within an ascending or descending branch of the circulation.

Another role of turbulent PBL-based circulations in convective initiation is to define sites at which deep

convective clouds form along a mesoscale boundary, such as one that arises from solenoidal circulations discussed earlier. Figure 9 diagrams deep convective cloud development that arises from the intersection of HCRs with a sea-breeze front.

See also

Boundary Layers: Convective Boundary Layer. **Buoyancy and Buoyancy Waves:** Theory. **Convective Storms:** Overview. **Dynamic Meteorology:** Waves. **Frontogenesis. Gust Fronts. Land–Sea Breeze. Mesoscale Meteorology:** Mesoscale Convective Systems. **Quasi-geostrophic Theory. Solitary Waves. Static Stability. Thermodynamics:** Moist (Unsaturated) Air; Saturated Adiabatic Processes. **Valley Winds. Weather Prediction:** Severe Weather Forecasting.

Further Reading

- Bluestein HB (1993) *Synoptic-Dynamic Meteorology in Midlatitudes, vol. II, Observations and Theory of Weather Systems*. New York: Oxford University Press.
- Crook NA (1996) The sensitivity of moist convection forced by boundary layer processes to low-level thermodynamic fields. *Monthly Weather Review* 124: 1767–1785.
- Emanuel KA (1994) *Atmospheric Convection*. New York: Oxford University Press.
- Holton JR (1992) *Introduction to Dynamic Meteorology*. New York: Academic Press.
- Iribarne JV and Godson WL (1981) *Atmospheric Thermodynamics*. Dordrecht: D. Reidel.

Kessler E (1986) *Thunderstorms: A Social, Scientific, and Technological Documentary, vol. 2, Thunderstorm Morphology and Dynamics*. Norman, OK: University of Oklahoma Press.

Pielke RA and Segal M (1986) Mesoscale circulations forced by differential terrain heating. In: Ray PS (ed.) *Mesoscale Meteorology and Forecasting*, pp. 516–548. Boston: American Meteorological Society.

Schaefer JT (1986) The dryline. In: Ray PS (ed.) *Mesoscale Meteorology and Forecasting*, pp. 549–572. Boston: American Meteorological Society.

Simpson JE (1997) *Gravity Currents in the Environment and the Laboratory*. Cambridge: Cambridge University Press.

Stull RB (1988) *An Introduction to Boundary Layer Meteorology*. Dordrecht: Kluwer Academic.

CORIOLIS FORCE

D W Moore, Pacific Marine Environmental Laboratory, Seattle, WA, USA

Copyright 2003 Elsevier Science Ltd. All Rights Reserved.

Introduction

The Coriolis force arises when Newton's equations of motion are written in a rotating coordinate system. It is named for Gaspard Gustave de Coriolis (1792–1843). His studies of dynamical problems associated with rotating machinery were presented to the Académie des Sciences in Paris in 1831.

All of the terms in the equations of motion related to the Coriolis force were actually included in the tidal equation of P. S. Laplace, published in 1775 and 1776, and repeated in Book IV of his *Treatise on Celestial Mechanics*, published in 1799.

Newton's equation of motion for a particle is

$$m \frac{d\vec{v}}{dt} = \vec{F} \quad [1]$$

where m is the mass of the particle, $\vec{v} = d\vec{r}/dt$ is the velocity of the particle, \vec{r} is the position vector, and d/dt is the time derivative following the motion of the particle. The quantity $\vec{a} = d\vec{v}/dt$ is the acceleration. This equation holds in an inertial reference frame, fixed with respect to the 'fixed' stars.

But the Earth on which we live rotates at a nearly constant rate about an axis whose direction is more or less fixed in inertial space. We denote the Earth's rotation vector by $\vec{\Omega}$, so $\Omega = |\vec{\Omega}|$ is the rotation rate. The direction of $\vec{\Omega}$ points from the South Pole to the North. The Earth rotates once each sidereal day, which is about 8.62×10^4 solar seconds. So the Earth's rotation rate is $\Omega = 7.29 \times 10^{-5} \text{ s}^{-1}$.

The motions of the atmosphere and the oceans are generally described in a coordinate system which rotates with the Earth. For example, longitude, latitude, and height above a reference geopotential surface form a convenient rotating system. Because

the Earth is rotating, it bulges at the Equator and is flattened at the poles. The reference geopotential includes both the gravitational and centrifugal potential, so the reference surface is not quite spherical. The Earth's equatorial radius exceeds the polar radius by about 21 kilometers. The shape of the geopotential and the Coriolis force both depend on the Earth's rotation rate.

Derivation of the Coriolis Force

Consider two coordinate systems, one of which is inertial, fixed with respect to the fixed stars, and the other rotating with angular velocity $\vec{\Omega}$. We use a prime to denote a quantity as viewed in the rotating frame and use unprimed quantities to denote the inertial frame. Let \vec{q} be a fixed vector in the inertial frame, so that

$$\frac{d\vec{q}}{dt} = 0 \quad [2]$$

Viewed in the rotating frame, \vec{q}' appears to rotate with angular velocity $-\vec{\Omega}$ in the direction opposite to the rotation of the coordinate system. So its apparent velocity in the rotating system is $-\vec{\Omega} \times \vec{q}'$, and we must add $+\vec{\Omega} \times \vec{q}'$ to this apparent velocity to bring it to zero. We are thus led to the rule

$$\frac{d}{dt} \vec{q} = \frac{d}{dt'} \vec{q}' + \vec{\Omega} \times \vec{q}' \quad [3]$$

where the terms on the left are viewed in the inertial frame and those on the right in the rotating frame. Furthermore, this same result, eqn [3], holds even if the left-hand side is not zero.

Consider a particle with position vector \vec{r} in the inertial frame and \vec{r}' in the rotating frame. The velocity is given by

$$\vec{v} = \frac{d\vec{r}}{dt} = \frac{d\vec{r}'}{dt'} + \vec{\Omega}' \times \vec{r}' = \vec{v}' + \vec{\Omega}' \times \vec{r}' \quad [4]$$